Hot-electron lifetimes in metals: A combined *ab initio* calculation and ballistic electron emission spectroscopy analysis

Florian Ladstädter,[1] Pilar F. de Pablos,[2] Ulrich Hohenester,[1] Peter Puschnig,[1] Claudia Ambrosch-Draxl,[1]
Pedro L. de Andrés,[3] Francisco J. García-Vidal,[2] and Fernando Flores[2]
[1]*Institut für Theoretische Physik, Karl–Franzens–Universität Graz, Universitätsplatz 5, 8010 Graz, Austria*
[2]*Departamento de Física Teórica de la Materia Condensada, U. Autónoma de Madrid, 28049 Madrid, Spain*
[3]*Instituto de Ciencia de Materiales (CSIC), Cantoblanco, 28049 Madrid, Spain*
(Received 9 May 2003; published 21 August 2003)

A first-principles analysis of ballistic electron emission spectroscopy (BEES) is used to extract hot-electron lifetimes in metals. The lifetimes are computed within an *ab initio* framework based on density-functional theory and the *GW* approximation, and are used in a Keldysh Green function approach for the calculation of BEES currents. For the two prototypical systems Au/Si and Pd/Si, which exhibit a significantly different scattering dynamics, we find an excellent agreement with experiment, which allows an accurate determination of hot-electron lifetimes.

DOI: 10.1103/PhysRevB.68.085107 PACS number(s): 72.15.Lh, 68.37.Ef, 71.10.Ca, 71.15.Ap

An accurate knowledge of inelastic hot-electron lifetimes in metals is of paramount importance for the understanding of a variety of important physical and chemical phenomena, ranging from surface chemistry to the design of devices based on metal-semiconductor junctions. However, the experimental knowledge of hot-electron lifetimes $\tau(E)$ due to electron-electron scatterings is still far from being complete. This somewhat surprising situation stems from the difficulties to extract $\tau(E)$ from experiment, a procedure in which the various physical mechanisms at play are usually inextricably intertwined. For that reason, the more attractive experimental techniques are those which allow the most direct extraction of lifetimes: besides the older standard techniques of transport,[1] photoemission and inverse photoemission,[2] which, however, usually seem to overestimate lifetimes, in recent years two-photon photoemission (2PPE) Ref. 3 and ballistic electron emission spectroscopy (BEES) Ref. 4 have received increasing interest. In 2PPE, one measures electrons excited in a two-photon cascade process: first, hot electrons are created by a femtosecond laser pulse; after a given time delay, a second pulse excites those electrons which have not suffered an inelastic scattering. Detection of these ionized electrons is used to extract $\tau(E)$. Unfortunately, the underlying analysis still depends on a number of decisive material parameters and transport processes, e.g., on the interplay of intraband and interband excitations, the assumed amount of Drude absorption, Auger decay, and secondary electrons,[3,5] which substantially hampers a comprehensive theory for 2PPE including all these features. In contrast, in BEES hot electrons are not excited by optical means but are injected through a scanning-tunneling-microscope (STM) tip into a thin metallic layer deposited on a semiconductor substrate. For excess energies of the injected electrons slightly above the Schottky barrier, after passage through the metal film only those electrons which have not suffered an inelastic scattering can overcome the barrier at the metal-semiconductor interface, and are detected as the BEES current. The advantage of this technique, as compared to 2PPE, is the presence of the Schottky barrier which energetically filters all scattered and secondary electrons. This allows a rather direct extraction of lifetimes if a sufficiently sophisticated theory is applied to analyze the experimental data.

The first step in this direction was undertaken in Ref. 6 where we calculated BEES currents using a parametrized $\tau(E)$, and demonstrated the sensitivity of this method for the extraction of such transport parameters. In this paper, we proceed significantly further and improve upon two important points: first, we compute the hot-electron lifetimes within an *ab initio* framework based on density-functional theory (DFT) [linearized augmented plane waves (LAPW) basis[7]] and on the GW framework[8,9] and second, we carefully reexamine the tunneling process and abandon our previous restriction to consider only nearest-neighbor interactions. As will be discussed below, within this scheme, the whole BEES process of (1) tunneling, (2) transport through the metallic layer, and (3) transmission/reflection at the metal-semiconductor interface is now treated within a true first-principles manner, thus rendering BEES an ideal tool for the extraction of accurate $\tau(E)$ values. For the two prototypical Au/Si and Pd/Si systems,[10,11] we find an almost perfect agreement with experiment, which is a remarkable finding in view of the substantially different nature of inelastic scatterings in Au and Pd.

We start by calculating the *ab initio* lifetimes of metals. Our theoretical analysis follows the framework outlined by Echenique *et al.*[12] We start from DFT band structure calculations performed with the WIEN97 code[7] which provide us with the band structure E_n and wave functions $\phi_n(\boldsymbol{r})$, with n labeling the band index and wave vector. These results are used within the GW-approximation framework for the calculation of the self-energy,[13] whose imaginary part yields $\tau(E)$ according to (we use atomic units $e^2=m=\hbar=1$)[12]

$$\tau^{-1}(E_0)=\frac{1}{\pi^2}\sum_f \int_{BZ} d\boldsymbol{q} \sum_{\mathbf{GG}'} \frac{B^*_{0f}(\boldsymbol{q}+\boldsymbol{G})B_{0f}(\boldsymbol{q}+\boldsymbol{G}')}{|\boldsymbol{q}+\boldsymbol{G}|^2} \times \Im(-\epsilon^{-1}_{\mathbf{GG}'}(\boldsymbol{q},E_0-E_f)), \quad (1)$$

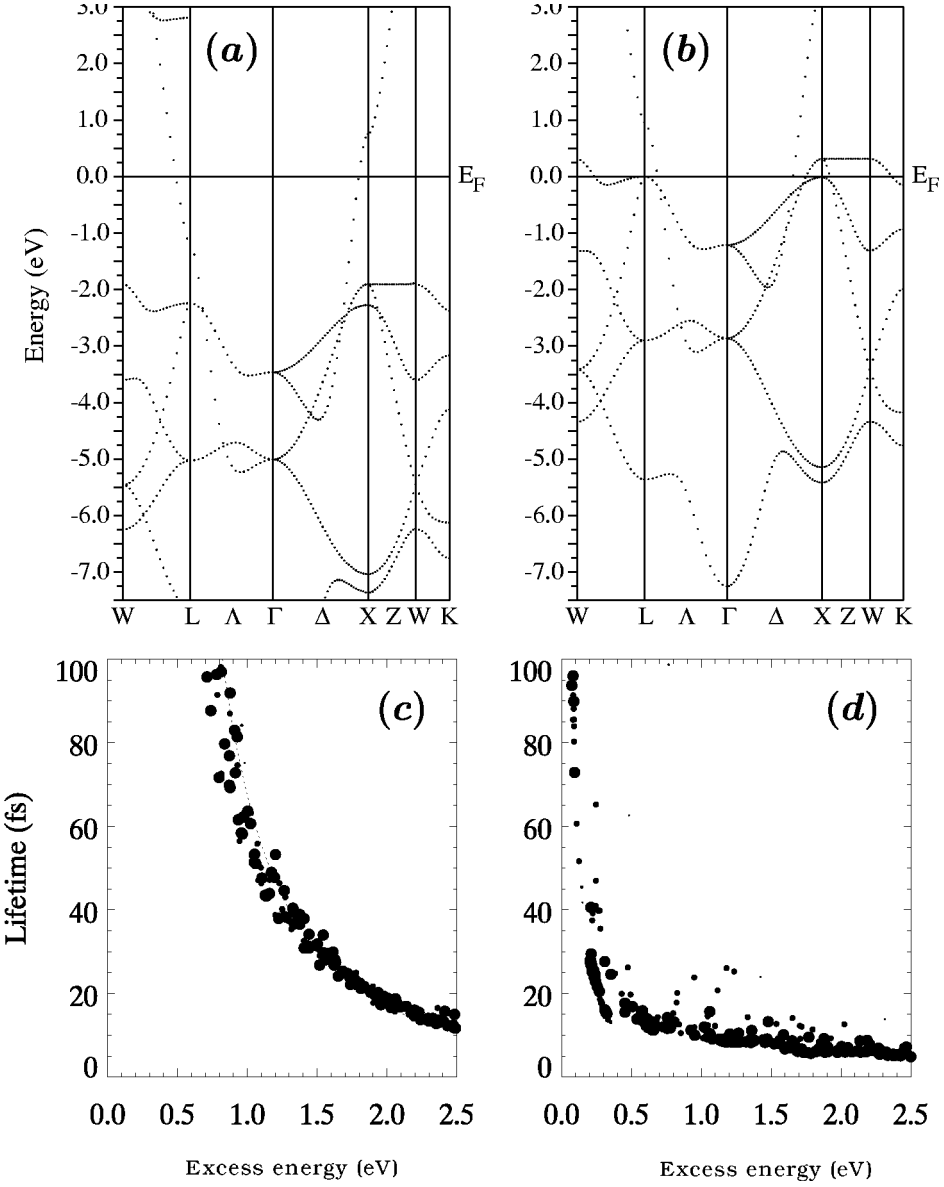

FIG. 1. Results of our LAPW-GW calculations: DFT band structure of (a) Au and (b) Pd; hot-electron lifetimes for (c) Au and (d) Pd, as computed from Eq. (1) for an equidistant k mesh with $20\times20\times20$ points.

with $\boldsymbol{q}$ being a wave vector within the first Brillouin zone BZ; $\boldsymbol{G}$ ($\boldsymbol{G}'$) a reciprocal lattice wave vector; 0 and f the initial and final states of the hot electron, respectively; B_{0f} the hot-electron overlap matrix elements for a given wave vector; and ϵ the dielectric function calculated within the usual random-phase approximation. We emphasize our use of the full LAPW wave functions for the calculation of the overlap matrix elements B, which we consider to be crucial for the analysis of metals with strongly localized d-band states. Details of the calculation of B, which turned out to be the computationally most costly part of our numerical approach, are published elsewhere.[14]

Figures 1(a,b) show results of our LAPW band structure calculations for Au and Pd, respectively. Here, the primary difference between the two materials is the different energetic position of the Fermi energy E_F: while in Au the d bands are located well below E_F, in Pd they cross the Fermi level. As will be demonstrated in the following, this different alignment of d bands and E_F results in completely different characteristics for $\tau(E)$. Figures 1(c,d) show $\tau(E)$ as computed from Eq. (1). Let us first concentrate on the results for Au, Fig. 1(c). For all initial states, $\tau(E)$ nicely follows the energy dependence predicted by electron-gas theory, $\tau(E) \sim (E-E_F)^{-2}$ [dotted line in Fig. 1(c)], whereas the absolute value of $\tau(E)$ turns out to be about three times larger, as predicted by the electron-gas theory.[15] This finding is in agreement with the results of Campillo *et al.*[16] and is attributed to genuine band structure effects. Furthermore, a closer analysis of our results reveals only minor importance of dynamic screening and of local-field effects; the latter point is in contradistinction to the pseudopotential calculations of Ref. 16 and clearly highlights the importance of using a most realistic wave function description for the calculation of $\tau(E)$ in transition metals. Next, we turn to the discussion of the Pd hot-electron lifetimes, Fig. 1(d), which exhibit an entirely different energy dependence that is almost constant over a wide range of initial energies $E_0 \sim 0.2$–2.5 eV. This surprising result is attributed to the d bands around E_F, and

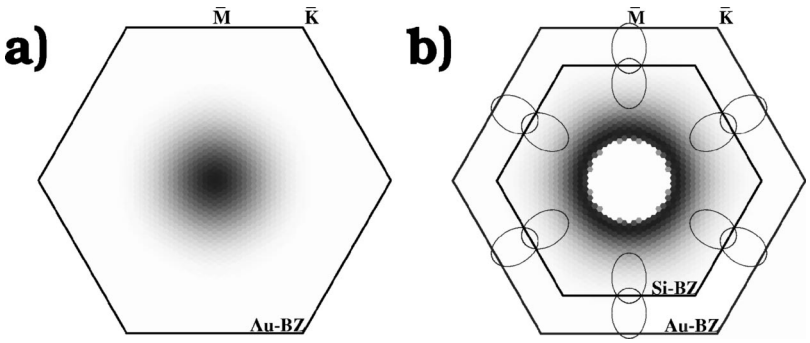

FIG. 2. (a) Tunneling current distribution inside the Au BZ and (b) corresponding current distribution reaching the Au/Si interface (Si BZ and the projected conduction-band ellipsoids are shown for reference). Both distributions are computed for $V_t = 1.2$ eV.

can be understood qualitatively as follows (see Zarate *et al.*[17,18] for a related discussion): because of the narrow energy width Δ of these bands [see Fig. 1(b)], the mean energy exchanged in an inelastic scattering is approximately Δ, irrespective of the initial hot-electron energy, which results in a constant $\tau(E)$; in contrast, the paraboliclike dispersion of Au leads to a $(E-E_F)$ increase of the number of scattering partners and of the phase space of final states, which results in the aforementioned electron-gas behavior of $\tau(E)$. It is noteworthy that these simple arguments can only provide a qualitative picture; detailed *ab initio* calculations are indispensable for obtaining accurate $\tau(E)$ values (as also evidenced by the dominant role of dynamic screening and local-field effects on $\tau(E)$ in Pd, which will be discussed elsewhere).

In the second step, we use our *ab initio* lifetimes $\tau(E)$ for the calculation of BEES currents. We follow the framework presented in Refs. 6,19 and calculate the BEES current I_{BEES} as a function of tip voltage V_t, according to:

$$I_{\mathrm{BEES}}(V_t) = \int_{V_b}^{V_t} dE \int_{BZ} d\boldsymbol{k}_{\parallel} I_b(E,\boldsymbol{k}_{\parallel} V_t) T(E,\boldsymbol{k}_{\parallel}) S(E). \quad (2)$$

Here the various terms can be associated to the different steps of the usual four-step BEES model:[20,21] (1,2) $I_b(E,\boldsymbol{k}_{\parallel};V_t)$, the current distribution of injected electrons with energy E, and parallel wave vector $\boldsymbol{k}_{\parallel}$ reaching the interface (see below); (3) $T(E,\boldsymbol{k}_{\parallel})$ the two-dimensional quantum-mechanical transmission coefficient at the Schottky barrier[19] (with barrier height V_b); and (4) $S(E)$, a factor accounting for phonon backscattering in Si of carriers that have successfully overcome the barrier (see Refs. 6,19 for our parametrization of $S(E)$ based on complementary ensemble-Monte-Carlo simulations).

The object of central importance in our BEES analysis is the current distribution $I_b(E,\boldsymbol{k}_{\parallel};V_t)$ at the metal-semiconductor interface. This distribution is computed within a nonequilibrium Green's functions formalism[19] that includes band structure effects by means of a tight-binding parametrization.[22] Firstly, if we neglect the multiple reflections at the metallic layer, the BEES current can be expressed as:[19]

$$I_b^{(1)}(E,\boldsymbol{k}_{\parallel}) = \frac{4e}{\hbar} \Im \mathrm{Tr}(\hat{G}^A_{1,m-1}(E,\boldsymbol{k}_{\parallel}) \hat{V}_{m-1,m} \hat{G}^R_{m1}(E,\boldsymbol{k}_{\parallel}) \times \hat{V}_{10}(\boldsymbol{k}_{\parallel}) \hat{\rho}_{00}(E) \hat{V}_{01}(\boldsymbol{k}_{\parallel})), \quad (3)$$

where $\hat{G}^R_{ij}$ ($\hat{G}^A_{ij}$) is the retarded (advanced) Green's function and $\hat{V}_{ij}$ the hopping matrix element connecting layers i and j in the metal; layer 1 and m correspond to surface and interface, respectively, and 0 denotes the last atom of the STM tip (we assume that only one atom in the tip is active in the tunneling process) which has a density of states $\hat{\rho}_{00}(E)$; and finally, the trace extends over our tight-binding basis. The hot-electron lifetimes are included in all Green's functions as an optical potential $\eta(E) = \hbar/2\tau(E)$, which causes an attenuation of the BEES current in accordance with the inelastic nature of electron-electron scatterings and the acting of the Schottky barrier as an energy filter. Note that no difficulties arise at this point due to our tight-binding parametrization[22] (which is obtained from *ab initio* calculations), since the hot-electron propagation is a pure band structure effect which is well described by means of $\hat{G}^{R,A}$ in Eq. (3). We finally emphasize that our present analysis completely neglects quasi-elastic scatterings in the metallic layer, e.g., electron-phonon interactions, an approximation only valid for thin films (see Refs. 19,23 for a detailed discussion of phonon scattering).

For thin metallic films, the BEES current is noticeably influenced by electrons which are reflected multiple times between surface and interface.[10] In such processes, the quality of the metal-semiconductor interface is of central importance: quite generally, for high quality, $\boldsymbol{k}_{\parallel}$ is conserved at interface scatterings, resulting in *specular reflection*, whereas for low quality there is no $\boldsymbol{k}_{\parallel}$ conservation and *diffuse reflection* occurs.[24,25] For our present study, we assume specular reflection for the high-quality Au/Si(111) interface (in accordance with experimental[26] and theoretical[19,23] evidence) whereas for Pd/Si we assume diffuse reflection.[11] Within our Green's function approach, for specular reflection the contribution to I_b from the ith passage is given by Eq. (3) when replacing m by $(2i+1)m$. For diffuse reflection electrons scattered after the first passage exhibit a random $\boldsymbol{k}_{\parallel}$ distribution, which can be simulated by using a uniform initial tunneling current distribution in $\boldsymbol{k}_{\parallel}$ space.

The second important improvement of this paper concerns our description of the tunneling process, in which we abandon our previous restriction of interactions between tip and a single atom in the metallic layer, but now allow for all possible tunneling paths. Hence, in real space, $\hat{V}_{01}(\boldsymbol{R}_{1i})$ becomes a matrix linking different sites in the surface layer $\boldsymbol{R}_{1i}$ with the tip-apex atom 0; the distance dependence of these matrix elements is computed within the Wentzel-Kramer-

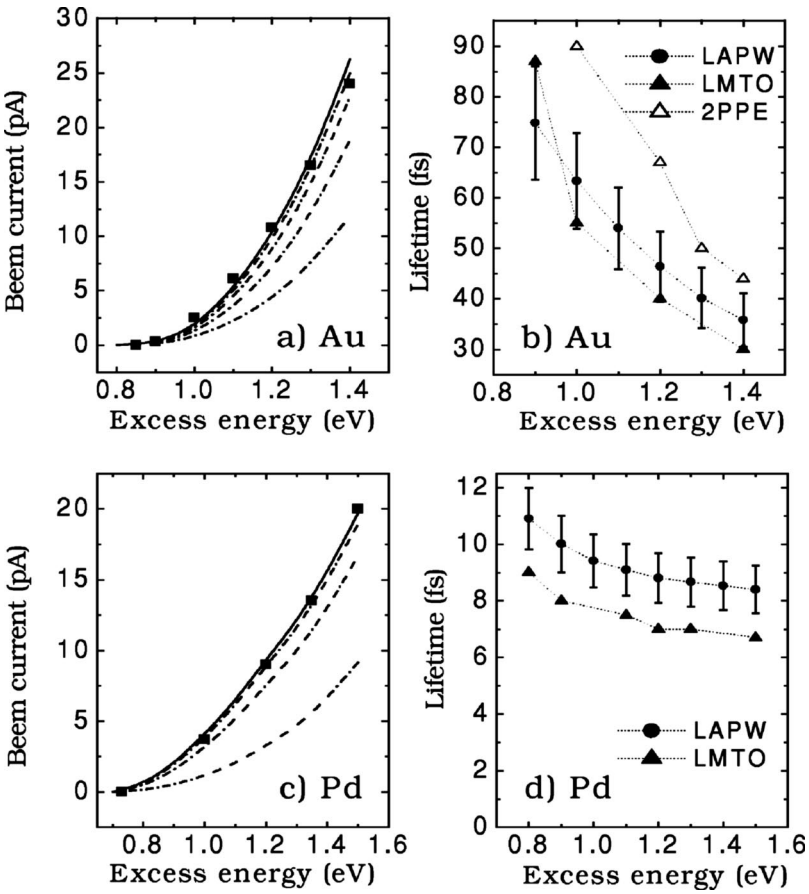

FIG. 3. $I_{\mathrm{BEES}}(V_t)$ spectra for (a) a 75 Å Au film deposited on Si(111) (Ref. 10) and (c) a 46 Å Pd film deposited on Si(111) (Ref. 11). Solid squares (lines) correspond to experiment (theory). Dashed-dotted lines show the accumulative contributions for different numbers of internal reflections. Panels (b) and (d) compare $\tau(E)$ computed in this work with values derived from linear muffin-tiv orbital (LMTO) calculations (Refs. 18,30) and two photon photoemission (2PPE) experiments (Ref. 5). Error bars for Au data (panel b) account for the variations in τLAPW needed to obtain perfect agreement with BEES experimental spectra (panel a, solid squares) whereas for the case of Pd (panel d), these error bars reflect changes in τLAPW required to fit experimental data reported for different metal thicknesses (Ref. 11).

Brillouin (WKB) approximation for the interface potential presented in Ref. 27, and we finally obtain $\hat{V}_{01}(\boldsymbol{k}_{\parallel}) = \Sigma_{\boldsymbol{R}_{1i}} \hat{V}_{01}(\boldsymbol{R}_{1i}) \times e^{i\boldsymbol{k}_{\parallel}\boldsymbol{R}_{1i}}$. From this analysis, we make the following important observations: first, the magnitude of $\hat{V}_{01}(\boldsymbol{R}_{1i})$ decreases rather slowly with distance (e.g., only by a factor of ~ 2 between first- and second-nearest neighbors) Ref. 31; second, the more the atoms are involved in the (real-space) tunneling process, the narrower the current distribution in $\boldsymbol{k}_{\parallel}$ space becomes. This is clearly shown in Figs. 2(a,b) for the tunnel distribution at the surface and interface, respectively, which should be compared to the broad $\boldsymbol{k}_{\parallel}$ distributions of our previous work[6] [the missing current contribution around $\boldsymbol{k}_{\parallel} \cong 0$ is due to the Au propagation gaps along (111), Ref. 19,28].

Figure 3(a,c) shows our calculated BEES currents in comparison with the experimental data of Refs. 10,11 for Au/Si and Pd/Si, respectively. We observe excellent agreement between theory (solid lines) and experiment (symbols) for both the material systems, which we consider a remarkable finding in view of the *first-principles* character of our analysis (i.e., no fitted values) and of the entirely different scattering dynamics in Au and Pd. In Fig. 3(c) we show the BEES spectrum for 46 Å of Pd on Si(111); the very good agreement gives us strong confidence in our approach, in particular since our BEES description is directly adopted from our older Au/Si work.[6,19,28] with the improvement of more realistic tunneling injection and the only exception of diffuse interface scattering, which we consider inevitable in view of the poor Pd/Si interface quality.[11] Taking into account multiple reflections at the interface, we reproduce the experimental data[11] using the lifetime values computed in the *ab initio* LAPW-GW calculation. Moreover, using our calculated values, we found agreement even for different Pd thicknesses with discrepancies of 10-20% when compared to *I-V* experimental curves as reported in Ref. 11 [see error bars in Fig. 3(d)]. On the other hand, the agreement for Au/Si is also very good. In Fig. 3(a) we show the BEES spectrum for 75 Å of Au on Si(111). Note that in previous BEES analysis, a substantially smaller $\tau(E)$ was needed to obtain agreement with experiment.[10] The small value of the BEES current, compared with the current injected from the STM tip ($1nA$) is not just due to the attenuation caused by electron-electron scatterings but indicate that an additional mechanism must be at play. Here, the most likely candidate is the aforementioned narrow $\boldsymbol{k}_{\parallel}$ distribution (that we did not take into account before) together with a strong degree of $\boldsymbol{k}_{\parallel}$ conservation at interface reflections/transmissions. In this situation, only a small portion of electrons, only those with appropriate energy and parallel momentum [see ellipses in Fig. 2(b)], can enter into the semiconductor. Finally, in Figs. 3(b,d) we compare our calculated hot-electron lifetimes to other experimental and theoretical values reported in the literature. Quite generally, all theoretical work has been based on density-functional theory within the local-density approximation, but different basis sets have been used, e.g., plane waves and norm-conserving pseudopotentials,[8,29] or linear muffin-tin or-

bitals (LMTO).[18] Comparing the latter LMTO $\tau(E)$ values with the present LAPW results, we observe a nice agreement for Au but a discrepancy of about 20% for Pd. We attribute this discrepancy to our improved description of the full potential, in contrast to the atomic sphere approximation of the LMTO method. As regards the experimental 2PPE lifetimes reported for Au, we observe approximately 40% larger values in comparison to our theoretical results. The origin of this discrepancy, which has been already noted in the literature, is not completely clear, but is probably related to the lack of a sufficiently sophisticated theoretical analysis comprising all relevant details.

In conclusion, we have presented a *first-principles* analysis of hot-electron lifetimes for Au/Si and Pd/Si. We have computed them within a LAPW-GW framework, and have used these values in a Keldysh Green's function approach for the calculation of BEES currents. Excellent agreement between experiment and theory has been found for both Au/Si and Pd/Si, which we consider to be a remarkable finding in view of the different nature of scatterings in Au and Pd. We thus believe that BEES is an ideal tool for the extraction of accurate $\tau(E)$ values in metals, and hope that our work will provide stimulus for future experimental studies.

This work was supported in part by the Austrian-Spanish project ''Acciones Integradas 2000-2001'' Project No. (HU1999-8), Spanish CICYT under Contracts Nos. MAT2002-01534 and MAT2002-00395, and EU Diode Network HPRCN-CT-1999-00164.

[1] S. Sze, C. Crowell, and E. Labate, J. Appl. Phys. **37**, 2690 (1966).
[2] A. Goldmann, W. Altmann, and V. Dose, Solid State Commun. **79**, 511 (1991).
[3] H. Petek and S. Ogawa, Prog. Surf. Sci. **56**, 239 (1997).
[4] L.D. Bell and W.J. Kaiser, Phys. Rev. Lett. **61**, 2368 (1988).
[5] J. Cao, Y. Gao, H.E. Elsayed-Ali, R.J.D. Miller, and D.A. Mantell, Phys. Rev. B **58**, 10 948 (1998).
[6] K. Reuter, U. Hohenester, P.L. de Andres, F. Garcia-Vidal, F. Flores, K. Heinz, and P. Kocevar, Phys. Rev. B **61**, 4522 (2000).
[7] P. Blaha, K. Schwarz, and J. Luitz, *WIEN97, A Full Potential Linearized Augmented Plane Wave Package for Calculating Crystal Properties* (Universität Wien, Vienna, 1999).
[8] I. Campillo, V.M. Silkin, J.M. Pitarke, A. Rubio, E. Zarate, and P.M. Echenique, Phys. Rev. Lett. **83**, 2230 (1999).
[9] W.-D. Schöne, R. Keyling, M. Bandic, and W. Eckardt, Phys. Rev. B **59**, 5926 (1999).
[10] L.D. Bell, Phys. Rev. Lett. **77**, 3893 (1996).
[11] R. Ludeke and A. Bauer, Phys. Rev. Lett. **71**, 1760 (1993).
[12] P.M. Echenique, J.M. Pitarke, E.V. Chulkov, and A. Rubio, Chem. Phys. **251**, 1 (2000).
[13] F. Aryasetiawan and O. Gunnarson, Rep. Prog. Phys. **61**, 237 (1998).
[14] P. Puschnig and C. Ambrosch-Draxl, Phys. Rev. B **66**, 165105 (2002).
[15] J.J. Quinn, Phys. Rev. **126**, 1453 (1962).
[16] I. Campillo, J.M. Pitarke, A. Rubio, and P.M. Echenique, Phys. Rev. B **62**, 1500 (2000).
[17] E. Zarate, P. Apell, and P. Echenique, Phys. Rev. B **60**, 2326 (1999).
[18] V.P. Zhukov, F. Aryasetiawan, E.V. Chulkov, and P.M. Echenique, Phys. Rev. B **65**, 115116 (2002).
[19] P.L. de Andres, F.J. Garcia-Vidal, K. Reuter, and F. Flores, Prog. Surf. Sci. **66**, 3 (2001).
[20] M. Prietsch and R. Ludeke, Phys. Rev. Lett. **66**, 2511 (1991).
[21] M. Prietsch, Phys. Rep. **253**, 163 (1995).
[22] D.A. Papaconstantopulos, *Handbook of the Band Structure of Elemental Solids* (Plenum, New York, 1986).
[23] P.F. de Pablos, F.J. Garcia-Vidal, F. Flores, and P.L. de Andres, Phys. Rev. B **66**, 075411 (2002).
[24] L.J. Schowalter and E.Y. Lee, Phys. Rev. B **43**, 9308 (1991).
[25] D.L. Smith, E.Y. Lee, and V. Narayamurti, Phys. Rev. Lett. **80**, 2433 (1998).
[26] M.K. Weilmeier, W.H. Rippard, and R.A. Buhrman, Phys. Rev. B **59**, 2521 (1999).
[27] J.M. Pitarke, P.M. Echenique, and F. Flores, Surf. Sci. **127**, 261 (1989).
[28] F.J. Garcia-Vidal, P.L. de Andres, and F. Flores, Phys. Rev. Lett. **76**, 807 (1996).
[29] W. Schone, R. Keyling, M. Bandic, and W. Ekardt, Phys. Rev. B **60**, 8616 (1999).
[30] V.P. Zhukov, F. Aryasetiawan, A.V. Chulkov, I.G. de Guturbay, and P.M. Echenique, Phys. Rev. B **64**, 195122 (2001).
[31] In our calculations we consider for Au and Pd tunneling up to fourth-nearest neighbors of the scanning-tunneling-microscope tip.